Applied Physics Letters ARTICLE scitation.org/journal/apl

Black phosphorus field effect transistors stable in harsh conditions via surface engineering

Cite as: Appl. Phys. Lett. **117**, 111602 (2020); doi: 10.1063/5.0021335
Submitted: 9 July 2020 · Accepted: 22 August 2020 ·
Published Online: 17 September 2020

Bei Jiang,[1,2] Hao Huang,[3] Rui Chen,[3] Guoli Li,[1] Denis Flandre,[1,4] Da Wan,[5] Xue Chen,[6] Xingqiang Liu,[1,a)] Cong Ye,[2,a)] and Lei Liao[1,3]

AFFILIATIONS

[1]Key Laboratory for Micro-/Nano-Optoelectronic Devices of Ministry of Education, School of Physics and Electronics, Hunan University, Changsha 410082, China
[2]Faculty of Physics and Electronic Science, Hubei University, Wuhan 430062, China
[3]School of Physics and Technology, Wuhan University, Wuhan 430072, China
[4]The ICTEAM Institute, Université Catholique de Louvain, Louvain-la-Neuve 1348, Belgium
[5]School of Information Science and Engineering, Wuhan University of Science and Technology, Wuhan 430081, China
[6]State Key Laboratory of High Power Semiconductor Lasers, Changchun University of Science and Technology, Changchun 130022, China

[a)]**Authors to whom correspondence should be addressed:** liuxq@hnu.edu.cn and yecong@issp.ac.cn

ABSTRACT

Black phosphorus (BP) has potential for fabricating p-type transistors in ultra-thin 2D-material complementary circuits. However, as the synergetic effect of water and oxygen leads to performance degradation under an ambient atmosphere, it is urgent to develop a passivation strategy for robust stability. Herein, a scalable superhydrophobic passivation layer is designed to improve the stability of BP transistors, which consists of fluoroalkylsilane-coated titanium dioxide (TiO_2) nanoparticles. Due to the superhydrophobic property of the passivation layer, the BP transistors preserve intrinsic performance in extremely wet conditions, including humid air, water, HCl, and KOH. After 28 days in atmospheric conditions, the performance presents only 20% channel current degradation and the device can work even after 60 days. This work not only experimentally demonstrates robust stable BP transistors in harsh conditions but also provides a highly efficient and damage-free strategy to suppress the influence of water adsorption in atmospheric conditions for highly stable 2D materials devices.

Two-dimensional (2D) materials attract great interest for future high-performance electronics due to their unique electrical properties and atomically thin geometry. Black phosphorus (BP), with a suitable energy bandgap (0.3 ~ 2.0 eV) and relatively high mobility (~1000 $cm^2/V{\cdot}s$),[1,2] reveals an intrinsic p-type characteristic, which is essential to build low-power complementary circuits, along with common n-type 2D materials.[3–5] Nevertheless, the drastic oxidization of BP in air results in unstable electrical performance, which can be attributed to a synergetic effect of water and oxygen.[6–9] Many effective passivation strategies have been reported, including oxide layers via film deposition,[10–12] hexagonal boron nitride (*h*-BN) coverage with physical transfer,[13,14] and organics encapsulation.[15–17] However, typical heterogeneous integration of film deposition processes, such as atomic layer deposition (ALD) and electron beam evaporation (EBE), usually lead to additional chemical disorders and defects in the interface, which degrade the intrinsic electrical performance.[16,18] The physical transfer of *h*-BN flakes is time-consuming and unscalable. Moreover, although many previously reported works focus on the organics encapsulation strategy for improved stability, charge transfer is typically involved between the organic and channel layers, resulting in a threshold voltage shift.[15–17] Due to the lack of the rational design of the organic encapsulated layer, the inevitable degradation of the organics in long-term gives rise to the invalidation of the encapsulated layer.[15] Therefore, the previously reported passivation strategies are not scalable or interacting with the channel layer, leading to degraded electrical performance. Moreover, the complex water conditions, either acidic or alkaline solutions, are also harsh for some cases. Therefore, a robust, scalable, and damage-free integration approach is essential for delivering high-performance BP devices.

Herein, we report BP field-effect transistors (FETs) with long-term stability in harsh conditions (i.e., a relative humidity of 60%

around 35 °C), in which a superhydrophobic protection layer eliminates the influence of moisture. The passivation layer consisting of fluoroalkylsilane-coated TiO_2 nanoparticles is fabricated via the dip-coating approach. Compared with conventional fabrication processes, potentially aggressive for BP, the solution process is a low-energy and harmless integration strategy, which does not degrade the BP surface. The superhydrophobic passivation layer ensures improved stability of BP transistors against water, hydrochloric acid (HCl), and KOH under an ambient atmosphere. Moreover, the performance variation is below 20% after 28 days in moist air conditions, and the devices still work even after 60 days of exposure in atmospheric conditions. Moreover, this strategy offers a superhydrophobic protection layer for other highly stable 2D material transistors against water-based harsh threats and retains the device intrinsic electrical properties in ambient conditions.

Figure 1(a) shows schematics of the BP transistors with 1*H*, 1*H*, 2*H*, 2*H*-perfluorooctyltriethoxysilane (PFOTES)-coated TiO_2 nanoparticles as the protection layer. The nanoparticles are first dispersed in 3-ethoxy-1,1,1,2,3,4,4,5,5,6,6,6-dodecafluoro-2-trifluoromethylhexane (HFE-7500),[19] which is used as the precursor to fabricate the protection layer [Fig. 1(a-i)]. The BP flakes are mechanically exfoliated and transferred onto p^+-Si wafers with a 300 nm SiO_2 dielectric layer. The channel length ($L_{ch} = 3\ \mu m$) is defined by e-beam lithography and the Cr/Au (15 nm/50 nm) electrodes are deposited by thermal evaporation, as shown in Fig. 1(a-ii). The BP FET is finally coated by the protection layer, which is assembled using a dip-coating method [Fig. 1(a-iii)]. More fabrication details are provided in the supplementary material. Compared with previously reported "high-energy" deposition strategies, which usually involve atom or cluster bombardment, the process presented here is simple, scalable, and damage-free. The key functionality of this highly stable BP transistor is derived from the superhydrophobic layer,[19] which can isolate water from BP, while the BP channel layer maintains its intrinsic property. Raman spectra of the channel layer are shown in Figs. 1(b)–1(d) and S1. The Raman peaks of BP ($A^1_g \sim 362\ cm^{-1}$, $B_{2g} \sim 439\ cm^{-1}$, and $A^2_g \sim 467\ cm^{-1}$) are consistent with those of previous work,[9,15,16] and the peaks show a neglectable shift when covered with the passivation layer, indicating desirable interface quality between BP and the PFOTES-coated TiO_2 film. Moreover, in Figs. 1(b)–1(d), the Raman intensity and peak position of the protected BP channel layer remain essentially unchanged for 28 days in air, demonstrating the feasibility of the designed strategy. The detailed Raman spectra of Fig. 1(b) are shown in Figs. S1(a) and S1(b). In contrast, when the BP flake is exposed to the atmospheric conditions without the PFOTES-coated TiO_2 film protection, no characteristic peaks can be observed after only 3 days, as shown in Fig. S1(c). Figures 1(c) and 1(d) present the evolution of the characteristic peak position and intensity of the Raman spectra. The intrinsic BP displays a fast noticeable change in Raman spectra, which is consistent with the optical images of bare BP in air (Fig. S2). The protection layer covered BP apparently shows considerably improved stability when compared with the intrinsic BP flakes.

In order to further evaluate the protection characteristic of the TiO_2 layer, the surface coverages and hydrophobic experiments with different concentrations of TiO_2 solution are investigated. 8%, 15%, and 20% (weight percentage) solutions consist of 7.45 ml HFE-7500 and 1 g, 2 g, or 3 g TiO_2 nanoparticles (average diameter of < 100 nm) with the corresponding PFOTES, respectively. Figures 2(a), 2(b), and S3(a) are the scanning electron microscopy (SEM) images with different concentrations of PFOTES-coated TiO_2 nanoparticles on SiO_2 surfaces, respectively. When the concentration of nanoparticles is below 8 wt. %, a continuous compact passivation film cannot be formed and many pinholes are present, as shown in Fig. 2(a). In contrast, a uniform film can be obtained as the nanoparticle concentrations are 15% and 20%, as shown in Figs. S3(a) and 2(b). The TiO_2 nanoparticles agglomerate and form micrometer-size islands [Fig. S3(b)], which will further promote the agglomeration. A rough structure similar to the lotus leaf surface[20] is formed [Fig. S3(b)]. According to Cassie theory,[21,22] the droplets are partly lifted up by the surface roughness,

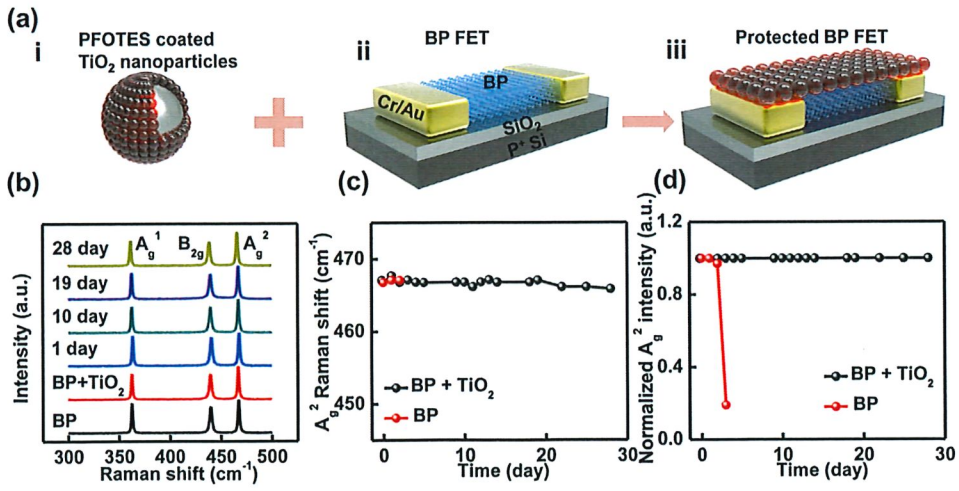

FIG. 1. Fabrication processes and Raman stability characterization. (a) Schematic illustrations of the BP transistor with PFOTES-coated TiO_2 nanoparticles as the protection layer. (b) Raman spectrum of the PFOTES-coated TiO_2 nanoparticle encapsulated BP in ambient conditions. The Raman shift (c) and the normalized peak intensity (d) of A^2_g at different ageing times. Black points represent PFOTES-coated TiO_2 nanoparticle encapsulated BP. Red points represent bare BP.

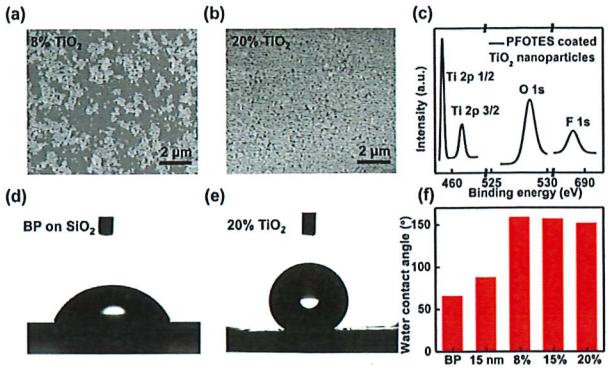

FIG. 2. Hydrophobicity characterization of PFOTES-coated TiO_2 layers. (a) and (b) SEM images for different concentration solutions with (a) 8% and (b) 20% PFOTES-coated TiO_2 nanoparticles on the SiO_2 surface. (c) XPS analysis of the PFOTES-coated TiO_2 layer. (d) and (e) Optical images of the water contact angle on (d) BP on SiO_2 and (e) 20% PFOTES-coated TiO_2 layer. (f) The change of the water contact angle on different layers. The water droplet is 10 μl. 15 nm represents the 15 nm TiO_2 film deposited by EBE.

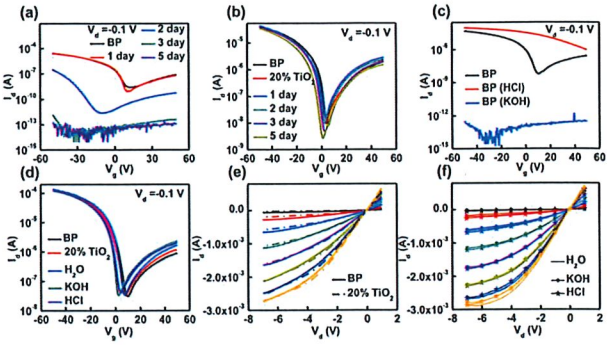

FIG. 3. Electrical stability measurements of PFOTES-coated TiO_2 nanoparticle encapsulated BP transistors. (a) Transfer curves for a bare BP transistor exposed to ambient air for different durations. (b) Transfer curves for a protected BP transistor exposed to moist air vs time. (c) Transfer curves of a bare BP transistor before and after exposure to HCl and KOH. (d) Transfer curves of a protected BP transistor with the PFOTES-coated TiO_2 nanoparticle layer before and after exposure to H_2O, HCl, and KOH for 10 s. (e) Output curves of BP transistors before and after protection. (f) Output curves of a BP transistor protected with the PFOTES-coated TiO_2 nanoparticle layer after exposure to H_2O, HCl, and KOH for 10 s ($V_g = 20$ V to -50 V in steps of -10 V).

which traps some air and forms a contact composite between solid, liquid, and gas. As a bit of air is trapped underneath the liquid, the contact area between droplets and the micrometer islands is reduced. Thus, the water cannot completely enter the gaps between the islands in the film, leading to enhanced hydrophobicity. As shown in Fig. 2(c), the chemical composition of TiO_2 nanoparticles after PFOTES modification is analyzed by x-ray photoelectron spectroscopy (XPS). Besides the Ti and O peaks of TiO_2, the F 1s peak is obviously observed, which indicates that the TiO_2 nanoparticles are coated with PFOTES.[19,23,24] PFOTES reduces the surface energy of TiO_2, leading to low affinity for water.[19,23,25–27] Due to the combined action of the rough surface and the low surface energy, the protection layer acquires a superhydrophobicity.[28] Thus, the water contact angle test shows that the PFOTES-coated TiO_2 film is more hydrophobic than the intrinsic BP on SiO_2. The water contact angles of the PFOTES-coated TiO_2 film are all $> 150°$ and the maximum can reach 159°, whereas the intrinsic BP shows a water contact angle of 66° [Figs. 2(d)–2(f) and S4(a)–S4(c)]. In contrast, without the combined action of the rough surface and the low surface energy, the 15 nm TiO_2 film deposited by EBE exhibits a low contact angle of 88°. The results indicate that the protection layer composed of PFOTES-coated TiO_2 nanoparticles can effectively protect BP from extremely wet conditions.

The superhydrophobic film composed of the PFOTES-coated TiO_2 nanoparticles is ideal for surface passivation of BP flakes, and the influence of the protection layer on the stability of BP transistors is investigated in Figs. 3(a)–3(f). The 20% solution is used to form a protection layer. The transfer characteristics (I_d-V_g) are measured at a fixed drain voltage (V_d) of -0.1 V. The BP transistors are directly exposed to atmospheric conditions with a relative humidity of 60% around 35 °C. In Fig. 3(a), the intrinsic BP transistor quickly does not work after 3 days, which can be attributed to the oxidation of the BP flake. In contrast, the BP transistors with the protection layer present desirable stability against the corrosion of atmosphere, and so the I_d-V_g curves indicate a negligible change, as shown in Fig. 3(b). The on-state current (I_{on}), on-off ratio (I_{on}/I_{off}), threshold voltage (V_{th}), and field-effect mobility (μ) closely coincide before and after exposure to moisture air for 5 days. To further ensure that the PFOTES-coated TiO_2 protection layer could be an alternative strategy to improve the electrical reliability of BP transistors against water-based threats, the evolution of the electrical performance of the BP transistors with and without the protection layer is investigated before and after exposure to various corrosive solutions, including H_2O (PH 6.7), HCl (PH 1.0), and KOH (PH 13.0). Figure 3(c) shows the drastic degradation of the intrinsic BP transistors after soaking in HCl solution for 10 s. Although I_{on} is increased, the on/off ratio is sharply reduced and V_{th} exhibits a remarkable positive shift. Meanwhile, after immersing into KOH solution for 10 s, I_{on} is below ~1 pA and the BP flake almost disappears (Fig. S5). The BP device is completely damaged before exposure to water, while the electrical characteristics of protected BP transistors are greatly maintained when they are exposed to various corrosive solutions [Figs. 3(d)–3(f)]. In Fig. 3(d), all electrical characteristics, such as I_{on}, I_{on}/I_{off}, V_{th}, and μ, do not have significant degradation. Figures 3(e) and f are the corresponding output characteristics (I_d-V_d) of Fig. 3(d). The output characteristic curves are measured by sweeping gate voltage (V_g) from 20 V to -50 V with an increment of -10 V. It is noted that the output curves of the BP transistor coated by TiO_2 after H_2O, HCl, and KOH immersion coincide with that of the original BP transistor, which excellently demonstrates the reliability of PFOTES-coated TiO_2 acting as the protection layer.

To further confirm the long-time electrical reliability of BP transistors in extremely wet conditions (i.e., relative humidity of 60% around 35 °C), on-state current and field-effect mobility are extracted to show changes over time [Figs. 4(a)–4(c) and S6(a) and S6(b)]. On-state current variation is exhibited by black points corresponding to the left Y-axis, and field-effect mobility variation is represented by red points corresponding to the right Y-axis. Serious performance

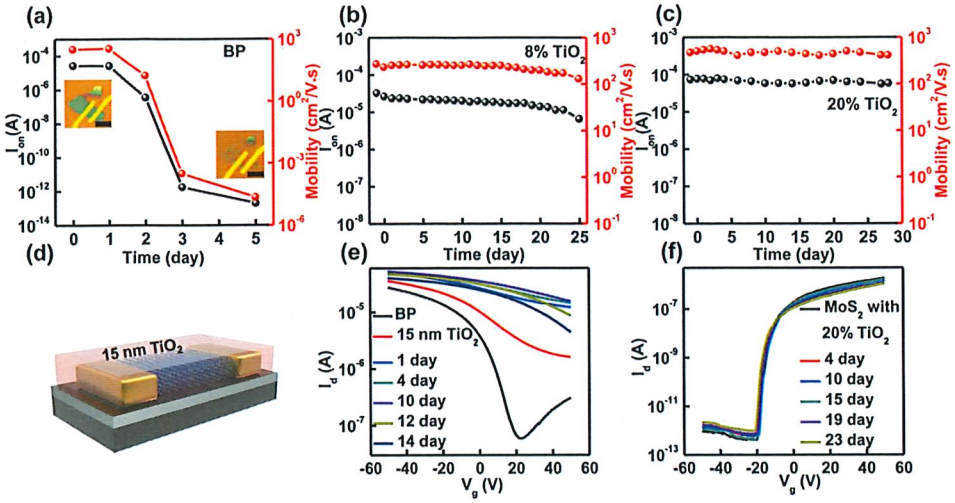

FIG. 4. Electrical stability measurements of bare and protected BP transistors. (a)–(c) The on-state current and mobility of BP transistors (a) without protection layer and with (b) 8% or (c) 20% PFOTES-coated TiO_2 nanoparticle encapsulation layers as a function of time at $V_d = -0.1$ V. The insets are optical images of the device taken at "day 0" and day 5, respectively. The scale bar is 9 μm. (d) A schematic of a BP transistor with 15 nm TiO_2 deposited by EBE. (e) Transfer curves for a BP transistor with the 15 nm TiO_2 EBE layer exposed to ambient air for different durations ($V_d = -0.1$ V). (f) Transfer curves for a MoS_2 transistor with the 20% PFOTES-coated TiO_2 nanoparticle layer exposed to ambient air vs time ($V_d = 0.1$ V).

damage is obviously seen in the intrinsic BP transistor, as shown in Fig. 4(a). The insets are optical images of the BP device taken on "0 day" and after 5 days, respectively. After 8% TiO_2 protection, the BP transistor can retain its electrical properties up to 25 days. However, due to the discontinuous protection film, the performance slowly reduces as time goes on [Fig. 4(b)]. When the protection film is uniform and compact for increasing TiO_2 concentrations, the electrical variations can almost display a horizontal linear trend. The horizontal tendency of Fig. 4(c) indicates that the performance variation over time is negligible and ignorable. The good electrical properties of $I_{on} \sim 79$ μA and $\mu \sim 572\,cm^2/V{\cdot}s$ are retained at more than 80% after 28 days, revealing the electrical stability of BP transistors with the TiO_2 protection layer. Although BP is sensitive to water for its large surface area, the PFOTES-coated TiO_2 nanoparticles prevent BP from oxidization thanks to the superhydrophobicity. The best BP transistors with 15% TiO_2 can be maintained up to 50 days, and the best record of 20% TiO_2 protected BP transistors is 60 days [Fig. S6(a) and S6(b)]. Compared with this damage-free method, typical processes, such as EBE, are aggressive and devastating. Figure 4(d) is the schematic of a BP transistor with the 15 nm TiO_2 film deposited by EBE. From the transfer curves shown in Fig. 4(e), the performance of the latter BP transistor is completely changed by the deposition process. Although this EBE TiO_2 film is useful for maintaining the electrical characteristics for a long period and although the unchanged electrical properties of the BP transistor after 15 nm TiO_2 deposition can be retained for 14 days, the EBE deposition is a high-energy assembly method that creates defects in the BP channel so that the device has better conductivity and loses its intrinsic on/off ratio.[18] Compared with this conventional aggressive fabrication process, the damage-free solution process is a physical transfer approach that could gently integrate PFOTES-coated TiO_2 on the BP surface without the creation of defects. Thus, the BP transistors with protection layers formed by PFOTES-coated TiO_2 can work with long-term stability in harsh conditions (i.e., a relative humidity of 60% around 35 °C).

A similar stability improvement is also observed in complementary MoS_2 n-type devices. Figure S6(c) and Fig. 4(f) show the back-gated transfer characteristics of MoS_2 transistors with a 3 μm channel length before and after PFOTES-coated TiO_2 encapsulation, respectively. The drain voltage is 0.1 V and the solution concentration is 20%. MoS_2 is a stable 2D material, which will not react with anything in air. Nonetheless, water and oxygen molecules can be adsorbed on the surface, leading to a right shift of threshold voltage and a reduction of on-state current of the unprotected device [Fig. S6(c)]. After 23 days of exposure in air, the on-state current is reduced from 4.54 μA to 0.83 μA and the field-effect mobility is depressed by 30%. The threshold voltage shifts by ~10 V to the right. These electrical variations confirm that the surface absorbate has a significant influence on intrinsic characteristics of MoS_2 transistors. Thus, MoS_2 materials also need surface passivation. In contrast to Fig. S6(c), the transfer curves of Fig. 4(f) show that the threshold voltages are little changed after a few days and on-state current change is neglected. The PFOTES-coated TiO_2 protection layer prevents water and oxygen molecules from adsorption on the surface of MoS_2, which enhances the performance stability of MoS_2 transistors allowing complementary logic operation with BP FETs.

In summary, we focused on increasing the long-term stability of BP transistors in extremely wet conditions, by introducing PFOTES-coated TiO_2 nanoparticles as a superhydrophobic protection layer, which eliminates the influence of moisture on the performance of BP transistors in the short and long terms. Compared with conventional aggressive fabrication processes, the BP channel is simply covered with the superhydrophobic protection layer with the dip-coating method.

Thus, the defect-free strategy and the superhydrophobic protection layer enable improved stability of BP transistors against water, HCl, and KOH. In addition, the performance variation is below 20% after 28 days in extremely wet conditions (i.e., relative humidity of 60% around 35 °C) and the devices still operate after 60 days. This method can also be utilized for other highly stable 2D materials such as MoS_2 to prevent channel materials from adsorbing moisture molecules and suppress the defects on channel surface. Therefore, the protection layer presented here allows 2D transistors[1–5,29,30] to stably operate under ambient conditions for practical applications.

See the supplementary material for the detailed Raman spectra, optical images, SEM images, and detailed water contact angle images; and additional electronic properties are available in the online version of this article.

AUTHORS' CONTRIBUTIONS

B.J. and H.H. contributed equally to this work.

We acknowledge the National Key Research and Development Program of Ministry of Science and Technology (Grant Nos. 2018YFA0703704 and 2018YFB0406603), the National Natural Science Foundation of China (Grant Nos. 61925403, 61851403, 61904129, 61811540408, 51872084, and 61704051), and the Strategic Priority Research Program of Chinese Academy of Sciences (Grant No. XDB30000000).

DATA AVAILABILITY

The data that support the findings of this study are available from the corresponding author upon reasonable request.

REFERENCES

[1]L. Li, Y. Yu, G. J. Ye, Q. Ge, X. Ou, H. Wu, D. Feng, X. H. Chen, and Y. Zhang, Nat. Nanotechnol. **9**, 372–377 (2014).
[2]H. Liu, A. T. Neal, Z. Zhu, Z. Luo, X. Xu, D. Tománek, and P. D. Ye, ACS Nano **8**, 4033–4041 (2014).
[3]S. P. Koenig, R. A. Doganov, L. Seixas, A. Carvalho, J. Y. Tan, K. Watanabe, T. Taniguchi, N. Yakovlev, A. H. Castro Neto, and B. Özyilmaz, Nano Lett. **16**, 2145–2151 (2016).
[4]G. C. Constantinescu and N. D. M. Hine, Nano Lett. **16**, 2586–2594 (2016).
[5]M. Engel, M. Steiner, and P. Avouris, Nano Lett. **14**, 6414–6417 (2014).
[6]J. Miao, S. Zhang, L. Cai, M. Scherr, and C. Wang, ACS Nano **9**, 9236–9243 (2015).
[7]W. Luo, D. Y. Zemlyanov, C. A. Milligan, Y. Du, L. Yang, Y. Wu, and P. D. Ye, Nanotechnology **27**, 434002 (2016).
[8]Y. Abate, D. Akinwande, S. Gamage, H. Wang, M. Snure, N. Poudel, and S. B. Cronin, Adv. Mater. **30**, e1704749 (2018).
[9]A. Favron, E. Gaufres, F. Fossard, A. L. Phaneuf-L'Heureux, N. Y. Tang, P. L. Levesque, A. Loiseau, R. Leonelli, S. Francoeur, and R. Martel, Nat. Mater. **14**, 826–832 (2015).
[10]D. K. Sang, H. Wang, Z. Guo, N. Xie, and H. Zhang, Adv. Funct. Mater. **29**, 1903419 (2019).
[11]Y. Y. Illarionov, M. Waltl, G. Rzepa, J. S. Kim, S. Kim, A. Dodabalapur, D. Akinwande, and T. Grasser, ACS Nano **10**, 9543–9549 (2016).
[12]J. S. Kim, Y. Liu, W. Zhu, S. Kim, D. Wu, L. Tao, A. Dodabalapur, K. Lai, and D. Akinwande, Sci. Rep. **5**, 8989 (2015).
[13]A. Avsar, I. J. Vera-Marun, J. Y. Tan, K. Watanabe, T. Taniguchi, A. H. Castro Neto, and B. Özyilmaz, ACS Nano **9**, 4138–4145 (2015).
[14]S. Gamage, A. Fali, N. Aghamiri, L. Yang, P. D. Ye, and Y. Abate, Nanotechnology **28**, 265201 (2017).
[15]D. He, Y. Wang, Y. Huang, Y. Shi, X. Wang, and X. Duan, Nano Lett. **19**, 331–337 (2019).
[16]X. Li, J. Wu, Y. Ye, S. Li, T. Li, X. Xiong, X. Xu, T. Gao, X. Xie, and Y. Wu, ACS Appl. Mater. Interfaces **11**, 1587–1594 (2019).
[17]D. Yue, D. Lee, Y. D. Jang, M. S. Choi, H. J. Nam, D. Y. Jung, and W. J. Yoo, Nanoscale **8**, 12773–12779 (2016).
[18]Y. Liu, J. Guo, E. Zhu, L. Liao, S. J. Lee, M. Ding, I. Shakir, V. Gambin, Y. Huang, and X. Duan, Nature **557**, 696–700 (2018).
[19]D. Yoo, Y. Kim, M. Min, G. H. Ahn, D. H. Lien, J. Jang, H. Jeong, Y. Song, S. Chung, A. Javey, and T. Lee, ACS Nano **12**, 11062–11069 (2018).
[20]W. Barthlott and C. Neinhuis, Planta **202**, 1–8 (1997).
[21]K. Kubiak, M. Wilson, T. Mathia, and P. Carval, Wear **271**, 523–528 (2011).
[22]A. B. D. Cassie and S. Baxter, Trans. Faraday Soc. **40**, 546–551 (1944).
[23]Y. Lu, S. Sathasivam, J. Song, C. R. Crick, C. J. Carmalt, and I. P. Parkin, Science **347**, 1132 (2015).
[24]Z. Song, J. Hrbek, and R. Osgood, Nano Lett. **5**, 1327–1332 (2005).
[25]C.-Y. Wang, H. Groenzin, and M. J. Shultz, Langmuir **19**, 7330–7334 (2003).
[26]Y. Lai, Y. Tang, J. Gong, D. Gong, L. Chi, C. Lin, and Z. Chen, J. Mater. Chem. **22**, 7420 (2012).
[27]T. Nishino, M. Meguro, K. Nakamae, M. Matsushita, and Y. Ueda, Langmuir **15**, 4321–4323 (1999).
[28]L. Feng, S. Li, Y. Li, H. Li, L. Zhang, J. Zhai, Y. Song, B. Liu, L. Jiang, and D. Zhu, Adv. Mater. **14**, 1857–1860 (2002).
[29]F. Wu, Q. Li, P. Wang, H. Xia, Z. Wang, Y. Wang, M. Luo, L. Chen, F. Chen, J. Miao, X. Chen, W. Lu, C. Shan, A. Pan, X. Wu, W. Ren, D. Jariwala, and W. Hu, Nat. Commun. **10**, 4663 (2019).
[30]M. S. Long, A. Y. Gao, P. Wang, H. Xia, C. Ott, C. Pan, Y. J. Fu, E. F. Liu, X. S. Chen, W. Lu, T. Nilges, J. B. Xu, X. M. Wang, W. D. Hu, and F. Miao, Sci. Adv. **3**, e1700589 (2017).